Lutetium coating of nanoparticles by atomic layer deposition

Moret, Josette L.T.M.; Griffiths, Matthew B.E.; Frijns, Jeannine E.B.M.; Terpstra, Baukje E.; Wolterbeek, Hubert T.; Barry, Seán T.; Denkova, Antonia G.; Van Ommen, J. Ruud

Citation (APA)
Moret, J. L. T. M., Griffiths, M. B. E., Frijns, J. E. B. M., Terpstra, B. E., Wolterbeek, H. T., Barry, S. T., Denkova, A. G., & Van Ommen, J. R. (2020). Lutetium coating of nanoparticles by atomic layer deposition. *Journal of Vacuum Science and Technology A: Vacuum, Surfaces and Films*, *38*(2), Article 022414. https://doi.org/10.1116/1.5134446

Important note
To cite this publication, please use the final published version (if applicable).
Please check the document version above.

Lutetium coating of nanoparticles by atomic layer deposition

Josette L. T. M. Moret, Matthew B. E. Griffiths (iD), Jeannine E. B. M. Frijns, Baukje E. Terpstra, Hubert T. Wolterbeek, Seán T. Barry (iD), Antonia G. Denkova, and J. Ruud van Ommen (iD)

COLLECTIONS

Paper published as part of the special topic on Special Topic Collection on Atomic Layer Deposition (ALD)
Note: This paper is part of the 2020 Special Topic Collection on Atomic Layer Deposition (ALD).

View Online   Export Citation   CrossMark

ARTICLES YOU MAY BE INTERESTED IN

Consistency and reproducibility in atomic layer deposition
Journal of Vacuum Science & Technology A **38**, 020804 (2020); https://doi.org/10.1116/1.5140603

Understanding chemical and physical mechanisms in atomic layer deposition
The Journal of Chemical Physics **152**, 040902 (2020); https://doi.org/10.1063/1.5133390

Atomic layer deposition of metals: Precursors and film growth
Applied Physics Reviews **6**, 041309 (2019); https://doi.org/10.1063/1.5087759

Lutetium coating of nanoparticles by atomic layer deposition

Josette L. T. M. Moret,[1,2] Matthew B. E. Griffiths,[3] ⓘD Jeannine E. B. M. Frijns,[2] Baukje E. Terpstra,[1]
Hubert T. Wolterbeek,[1] Seán T. Barry,[3] ⓘD Antonia G. Denkova,[1] and J. Ruud van Ommen[2] ⓘD

AFFILIATIONS

[1]Applied Radiation and Isotopes, Applied Sciences, Delft University of Technology, Delft 2629 JB, The Netherlands
[2]Product and Process Engineering, Applied Sciences, Delft University of technology, Delft 2629 HZ, The Netherlands
[3]Department of Chemistry, Carleton University, Ottawa, Ontario, K1S 5B6, Canada

Note: This paper is part of the 2020 Special Topic Collection on Atomic Layer Deposition (ALD).

ABSTRACT

Atomic layer deposition (ALD) is a versatile gas phase coating technique that allows coating of complex structured materials, as well as high-surface area materials such as nanoparticles. In this work, ALD is used to deposit a lutetium oxide layer on TiO_2 nanoparticles (P25) in a fluidized bed reactor to produce particles for nuclear medical applications. Two precursors were tested: the commercially available $Lu(TMHD)_3$ and the custom-made $Lu(HMDS)_3$. Using $Lu(TMHD)_3$, a lutetium loading up to 15 wt. % could be obtained, while using $Lu(HMDS)_3$, only 0.16 wt. % Lu could be deposited due to decomposition of the precursor. Furthermore, it was observed that vibration-assisted fluidization allows for better fluidization of the nanoparticles and hence a higher degree of coating.

Published under license by AVS. https://doi.org/10.1116/1.5134446

I. INTRODUCTION

Lutetium has various applications. For instance, lutetium oxide is used in semiconductor devices due to its favorable high dielectric constant,[1,2] as well as in catalysis because of its ability to reduce bandgap energy and hence increase the catalytic effect.[3] In the field of nuclear medicine, lutetium—specifically the radioactive isotope ^{177}Lu—is one of the most promising therapeutic radionuclides due to its favorable decay characteristics.[4,5] Upon radioactive decay, ^{177}Lu emits both a β^- particle and a gamma ray. The energy of the β^- particle (498 keV) is ideal for the treatment of (metastasized) tumors, while the gamma energy is suitable for imaging purposes, making ^{177}Lu a so-called theranostic (therapeutic and diagnostic) radionuclide. To ensure weekly patient treatment of various cancer types, hospitals are currently relying on weekly supplies of ^{177}Lu. However, hospitals prefer an "on demand" supply to ensure patient treatment that is independent of suppliers. Radionuclide generators are ideal for this purpose, providing not only "on demand" supply but usually also high specific activity (i.e., activity per unit mass), which is important to realize optimal therapeutic outcome.[6] A radionuclide generator typically consists of a material packed in a column holding the parent radioisotope. Upon radioactive decay of this parent radioisotope, a daughter radioisotope is formed. When eluting the radionuclide generator, the desired daughter radioisotope can be obtained, while the parent radioisotope remains on the column. In view of the extended use of ^{177}Lu, a radionuclide generator for this isotope is very much desired. However, the parent radionuclide ^{177m}Lu is chemically and physically identical to the daughter, so conventional separation techniques cannot be used. However, radiochemical properties can be exploited.[5,7] In order to make use of these radiochemical properties, the parent radionuclide should be strongly immobilized, so that upon decay only the ^{177}Lu is released and can be extracted. This process has been previously demonstrated by Bhardwaj et al.,[7] indicating that the yield depends on the stability of the parent-substrate complex. Furthermore, this process is most efficient when the released ^{177}Lu can escape from its environment; therefore, thin lutetium nanostructures are beneficial.

If we were to build such a radionuclide generator, aiming at one patient dose [7.4 GBq (Ref. 8)] per day, a coating of at least 32 wt. % Lu is required (supplementary material S4)[31] when considering a column elution efficiency of 80% and using 2 g of the column material coated with natural occurring lutetium. To obtain this coating, atomic layer deposition (ALD) can be used.

The advantage of using ALD is that a thin coating across the whole substrate can easily be fabricated due to the self-limiting behavior of the process. Additionally, the amount of lutetium deposited can be tuned based on the application, as the lutetium content will depend on the number of cycles applied. In their 2012 review, Miikkulainen et al.[9] reported three different Lu-containing precursors used for ALD of lutetium-containing materials, namely $[Lu((Me_3Si)C_5H_4)_2Cl]_2$,[10] $Lu(^iPrO)_3$,[11] and Lu$[N(SiMe_3)_2]_3$.[12] However, these precursors are not commercially available, which would be detrimental to practical implementation at a later stage. A fourth Lu-containing precursor, $Lu(TMHD)_3$, was reported by Roeckerath et al.[13] This precursor is commercially available and was used in combination with a La containing compound to deposit the mixed-metal oxide $LaLuO_3$. The process is carried out in vacuum and, like with the other Lu precursors reported, Si-wafers were used as the substrate. Wafers have a small specific surface area in comparison to nanoparticles, which limits the amount that can be deposited. For the preparation of a radionuclide generator, nanoparticles having large surface area are necessary in order to achieve the desired Lu loading while still preserving the thin layer morphology.

The goal of this study is to deposit insoluble lutetium nanostructures on larger TiO_2 nanoparticle supports using a fluidized bed reactor (FBR). In an FBR, the substrate nanoparticles are suspended in a gas flow from below the reactor chamber, allowing the particles to behave as if they are a liquid. FBRs allow for scale-up of the coating process and permit good solid–gas mixing[14] and good heat transfer.[15] The applicability of lutetium tris (2,2,6,6-tetramethyl-3,5-heptanedionato) $[Lu(TMHD)_3]$, lutetium tris hexamethyldisilazane $[Lu(HMDS)_3]$, and lutetium tris acetylacetonate $[Lu(acac)_3]$ in combination with the coreactants O_3 and NH_3 is investigated in this paper.

II. MATERIALS AND METHODS

A. Chemicals

Lutetium tris(2,2,6,6-tetramethyl-3,5-heptanedionato) $[Lu(TMHD)_3]$ was purchased from Strem chemicals (France). Lutetium trisacetylacetonate $[Lu(acac)_3]$ was purchased from ABC Chemicals (Germany). Both substrates used in this study, silica (Aerosil 130) and titania (P25), were obtained from Evonik industries and dried overnight at 120 °C before use. The carrier gas was 5.0 grade nitrogen. Ozone was produced with an ozone generator (Sanders C200) and synthetic air. NH_3 was obtained as mixture gas of 15 wt. % NH_3 in N_2 from Linde gas. All precursors were transferred into custom-made stainless steel bubblers under inert conditions (nitrogen atmosphere). $LuCl_3$ was purchased from Strem Chemicals USA and used as received. Lithium bis(trimethylsilylamide) was purchased from Sigma-Aldrich chemical company and was used as received.

B. Preparation of Lu(HMDS)₃

$Lu(HMDS)_3$ was prepared according to Bradley et al.[16] Under inert conditions, lithium bis(trimethylsilylamide) was dissolved in tetrahydrofuran and cooled. To this mixture, $LuCl_3$ was added, and after 24 h stirring at room temperature, all solvent was removed

under vacuum. The compound was then extracted to n-pentane and recrystallized three times before being purified by sublimation.

C. Thermogravimetric analysis

Thermogravimetric analysis (TGA) measurements were performed using a Mettler Toledo TGA apparatus. A temperature sweep from 20 to 800 °C was undertaken with a heating rate of 10 °C/min in a nitrogen flow of 0.1 l/min.

Additional TGA measurements were performed using a National instruments TGA instrument, under inert loading conditions. The temperature sweep was from 20 to 600 °C with a heating rate of 10 °C/min in a nitrogen flow of 0.06 l/min.

D. Coating

ALD was performed in a custom-made fluidized bed reactor (Fig. 1). The fluidized bed reactor consisted of a glass column with an internal diameter of 25 mm and a length of 500 mm mounted on a stainless steel windbox with a stainless steel distributer plate. On top of the column, a distributer plate and a metal chamber were also connected. The required dosing time for $Lu(TMHD)_3$ was calculated to be 23 min and $Lu(HMDS)_3$ to be 10 min. For the coreactants O_3 and NH_3, the dosing times were calculated to be 1.62 and 2 min, respectively. The precursor and the coreactant were alternatively fed into the reactor chamber from the bottom of the reactor using nitrogen as a carrier gas, separated by 10 min purge pulses. The carrier gas flow was 0.5 l/min (1.52×10^{-2} m/s).
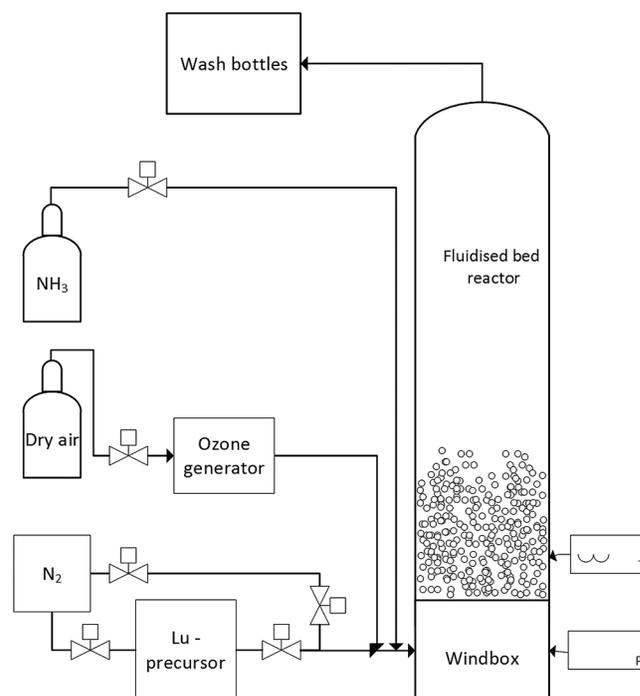
FIG. 1. Schematic representation of the fluidized bed reactor setup.

During the purge, an additional nitrogen flow of 0.1 l/min (0.30×10^{-2} m/s) was added. The lutetium precursor was kept in a custom-made stainless steel bubbler heated with a heating tape and was transported to the reaction chamber through heated stainless steel tubing. The fluidized bed was heated using an infrared lamp. The whole system was controlled using a PC with a custom-made LABVIEW program. The off gasses were washed with a series of wash bottles containing acidic water and kaydol oil and then an active carbon/HEPA filter.

E. Particle analysis

The lutetium content of the obtained particles was determined using instrumental neutron activation analysis (INAA) at the Reactor institute Delft. For this purpose, the particles were irradiated with a thermal neutron flux of 5×10^{16} n/s m^2, epithermal neutron flux of 9×10^{14} n/s m^2, and a fast neutron flux of 3.6×10^{15} n/s m^2 for 5 min. Using the obtained lutetium mass fraction, the layer thickness can be determined according to Valdesueiro et al.,[17]

$$\delta = \frac{\sqrt[3]{\frac{6}{\pi} \cdot V_{Lu_2O_3}^{1p} + d_{3,2}^3} - d_{3,2}}{2}$$

with

$$V_{Lu_2O_3}^{1p} = \frac{x_{Lu}}{1 - \frac{M_{Lu_2O_3}}{2M_{Lu}} \cdot x_{Lu}} \cdot \frac{M_{Lu_2O_3}}{2M_{Lu}} \cdot \frac{\rho_{TiO_2}}{\rho_{Lu_2O_3}} \cdot \frac{\pi}{6} \cdot d_{3,2}^3,$$

using a particle diameter of $d_{3,2} = 32.7$ nm and density of 4200 kg/m^3.[18] The density of Lu$_2$O$_3$ as deposited was assumed to be 9420 kg/m^3.[19] Dividing the layer thickness by the number of cycles gives the growth per cycle (GPC). Transmission electron microscopy (TEM) and scanning electron microscopy–electron dispersive spectroscopy (Jeol) were used to image the coating. The chemical environment of the deposited lutetium was characterized using x-ray photoelectron spectroscopy (XPS).

III. RESULTS AND DISCUSSION

A. Precursor and coreactant selection

The three potential precursors, Lu(acac)$_3$, Lu(TMHD)$_3$, and Lu(HMDS)$_3$, were first characterized using TGA to determine their applicability as ALD precursors. These TGA measurements were also used to calculate the vapor pressure of the compounds.[20] Considering the sensitivity of the precursors to air and moisture, measurements were carried in air as well as under a nitrogen atmosphere. Figure 2 shows indeed that air has a strong influence on the stability of the precursors. Lu(HMDS)$_3$ loaded under inert conditions shows a smooth mass loss curve during the analysis, while the same measurement in air resulted in low mass loss and a high residual mass.

A suitable precursor should have one single mass loss over the temperature range tested with virtually no remaining mass.[21] Therefore, based on these criteria, Lu(THMD)$_3$ is the most suitable precursor from the candidates tested, with a single mass loss
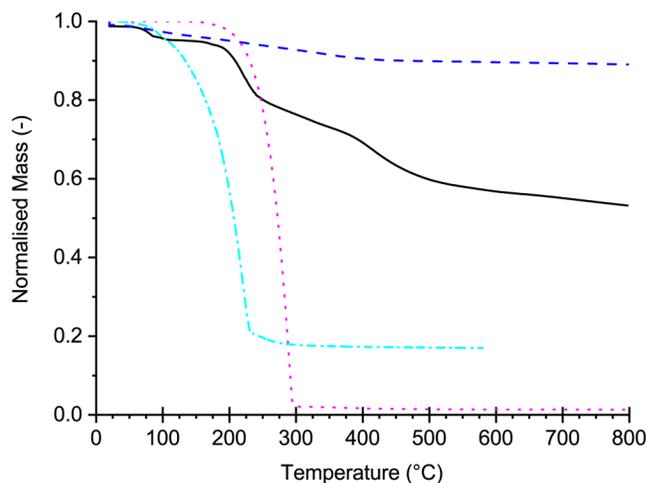
FIG. 2. Thermogravimetric analysis using nitrogen as a carrier gas of Lu(acac)$_3$ [solid line], Lu(TMHD)$_3$ [dotted line], and Lu(HMDS)$_3$ [dashed line] exposed to air during loading and Lu(HMDS)$_3$ [dashed-dotted line] loaded under inert conditions.

starting at 190 °C and virtually no mass remaining. However, even though Lu(HMDS)$_3$ has about 20% residual mass, it shows potential if kept under inert conditions, because of its single mass loss starting at 110 °C. The advantage of using Lu(HMDS)$_3$ over Lu(THMD)$_3$ is that Lu(HMDS)$_3$ can be used to deposit lutetium at lower temperatures. Lu(acac)$_3$, on the other hand, showed a stepwise mass loss, and the first mass loss is between 280 and 400 °C with the most significant mass loss at 310 °C. The second mass loss is between 800 and 850 °C with around 80% of the initial mass remaining, indicating that the compound decomposes when heated. Therefore, Lu(acac)$_3$ was determined to be unsuitable to use as an ALD precursor (Fig. 2).

Selection of a coreagent for deposition of a lutetium-containing film requires the ability to oxidize the precursor on the surface of the substrate. Initially, ozone was considered as a coreagent because it is known for its strong oxidizing potential. However, when an in water insoluble Lu layer is required, a different coreactant is needed. Lutetium is able to form several insoluble compounds like LuF and LuN.[22] Although HF is reported by Miikkulainen et al.[9] to make fluorides, it is strongly corrosive to the experimental setup and requires extra care when handled in the lab. Therefore, deposition of the nitride was preferred over the fluoride. The first experiments were carried out with ozone as a coreactant, as ozone was readily available.

B. Lutetium deposition

1. Lu(TMHD)$_3$ with O$_3$

The dosing time for Lu(TMHD)$_3$ was determined by calculating the dosing time for a single cycle based on the vapor pressure of Lu(TMHD)$_3$ at 210 °C ($P_{vap} = 42.7$ Pa). (See Sec. S1 in the supplementary material for vapor pressure calculation and Sec. S2 for

dose time calculation.)[31] These calculated dosing times were taken as the base case: 23 min of Lu(THMD)$_3$ and 0.81 min O$_3$ for 1.3 g titania P25 as the substrate. Titania P25 was chosen as a substrate for its strong metal–substrate interactions.[23] The expected Lu deposition for one cycle is 1.5 wt. %. The precursor pulses were separated by 10 min purge pulses. Then, several experiments with dosing times deviating from these times were conducted in order to determine whether there is self-limiting behavior. The lutetium loading on the particles was determined using INAA. The measurement uncertainty in the INAA measurements ranges from 2% to 4% (Fig. 3).

The first observation during the experiments is, due to the low mass of the nanoparticle agglomerates, some of the substrate material was sticking to the top of the column and reducing the bed volume, which might have led to earlier saturation. Tapping the column caused this cake to break down and fall back into the fluidized bed. Alternatively, the cake could be broken down by a small back pulse of nitrogen after every cycle. This caking could have an influence on the coating applied. As the cake was not fluidizing, a limited surface area was then exposed to the gas flow and could be coated. The influence on the lutetium loading of the particles in the bed was minimal, as we found that the cake had a comparable Lu loading to the particles in the bed.

Secondly, the coating process is delicate. Because of the relatively high precursor temperature, heat sinks could easily occur in the setup, even with extensive insulation. These heat sinks caused condensation of the precursor compound, leading to blockage of the system, which in turn reduced the nitrogen carrier gas flow and
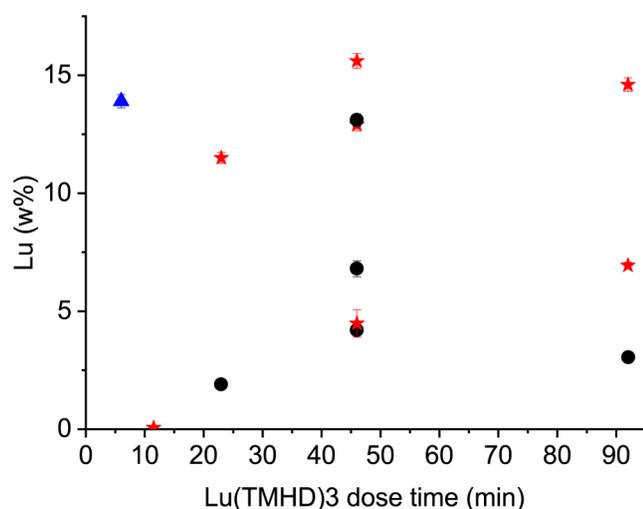
FIG. 3. Lu weight fraction [Lu (wt. %)] vs the dosing time of Lu(TMHD)$_3$. Precursor temperature was 210 °C, reactor temperature was 230 °C, and four cycles were applied using O$_3$ as coreactant. Red stars are obtained with vibration-assisted fluidization while black rounds refer to nonvibration-assisted fluidization. The blue triangle represents the experiment where 25 cycles were applied. Error bars represent the measurement uncertainty of INAA. Because of the spread in results, it was chosen to report the individual experiments rather than the average.

therefore the amount of Lu deposited. Also, large heat sinks in the windbox were sometimes observed. This resulted in large deposition of precursor in the windbox (Fig. S3).[31] On the other hand, hot spots in the bubbler caused by inhomogeneous heating of the bubbler could give unexpectedly high Lu loading on the particles. During the experiments, a temperature difference of up to 40 °C between the front and back of the bubbler was observed. Furthermore, during the experiments, it became clear that the state of the Lu(TMHD)$_3$ was influenced by its residence time in the heated bubbler. Upon refilling of the bubbler, it was observed that the remaining precursor had changed color (from white to pale yellow), indicating some amount of decomposition. During the initial TGA, this was not noticed because the decomposition is a rather slow process compared to evaporation. An additional TGA of the Lu(TMHD)$_3$ precursor that was heated up and cooled down showed that its temperature response had changed and some mass remained (Fig. S2),[31] indicating decomposition.

Figure 3 shows the deposition of lutetium as a function of the exposure time to Lu(TMHD)$_3$. It seems that for the experiments of 46 min and longer, self-limiting behavior occurs, as the amount of lutetium deposited goes to an asymptotic value, but the required long dosing times limited the number of experiments we could carry out. Typically, vibration assistance led to higher Lu loading. Vibration assistance allows for more efficient fluidization compared to nonvibration-assisted fluidization as it leads to effective breaking of interparticle forces.[24] This means that more bare surface area of the particles is exposed to the precursor, explaining the difference in Lu loading in both regimes. The corresponding GPC ranges from about 0.03 nm to about 0.11 nm. Compared to other lutetium ALD processes, this GPC is relatively low.[12] Nevertheless, it should be noted that those processes were operated under vacuum and using a different precursor; therefore, they are not directly comparable to the process described here. However, GPCs reported for other lanthanide (TMHD)$_3$ ALD processes[25] are comparable or are much lower.[26] The large deviation in the data can also be caused by the low vapor pressure of the precursor in combination with the gas flow rate. Possibly, the vapor above the precursor in the bubbler cannot saturate the headspace quickly enough during a pulse cycle, resulting in a decrease in precursor concentration over the duration of the Lu pulse. Keeping this in mind, the Lu precursor pulse was reduced to 6 min, while the number of cycles was increased (blue triangle in Fig. 3). The accumulated Lu(TMHD)$_3$ dose then was comparable to three cycles of 46 min. The deposited amount of Lu for 25 cycles at 6 min per cycle was similar to the deposition for 4 cycles at 46 min per cycle. Even though the accumulated Lu(TMHD)$_3$ pulse was shorter, the lutetium deposited was higher, which suggests that more and shorter pulses are indeed more effective for this low vapor pressure precursor. Furthermore, the GPC (Fig. 4) seemed to decrease when the number of cycles was increased. We attributed this mainly to the TiO$_2$ having more active surface sites for chemisorption than the overlayers of Lu$_2$O$_3$. The first reaction deposits more Lu when Lu(TMHD)$_3$ reacts with TiO$_2$ surfaces than subsequent reactions where Lu(TMHD)$_3$ reacts with Lu$_2$O$_3$ surfaces.[27–29] This might also be due to decomposition of the precursor during use, since increasing the number of cycles resulted in exposing the precursor to high temperature over a prolonged period of time.
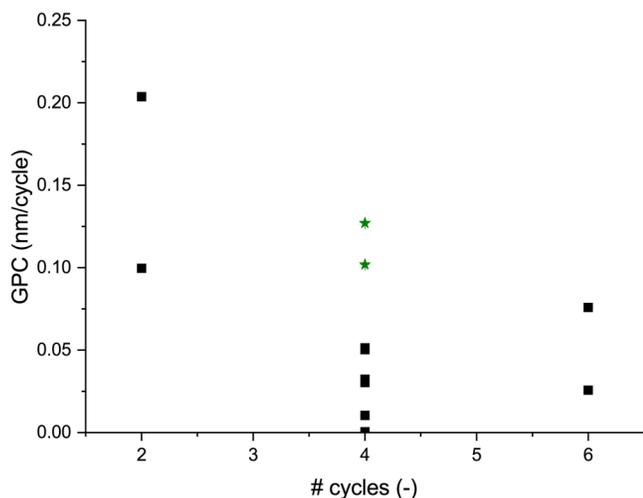
FIG. 4. GPC for precursor pulses $Lu(TMHD)_3$ and O_3 is 46 and 1.6 min, respectively. The layer thickness is derived from the amount of lutetium deposited determined by INAA. The squares are nonvibration assisted, while the stars are vibration assisted. Because of the widespread results, it was chosen to report the individual experiments rather than the average.

FIG. 5. TEM image of the coated particles. 46 min dose time of $Lu(TMHD)_3$ per cycle and four cycles, loading 13 wt. % Lu. The arrow indicates possible island formation.

The lutetium coating can be visualized using TEM; however, it is very difficult to get an accurate visualization of the coating within the 2 nm resolution or draw any hard conclusions. Because lutetium is a heavy element, it should appear darker in the image compared to the titania substrate. Using TEM, the layer thickness was estimated to be 0.75 nm and is therefore not comparable to the calculated layer thickness based on the INAA measurements (0.12 nm). However, the calculations are based on the assumption that a uniform layer is achieved. Due to agglomeration, it is possible that at some places a thicker coat resulted, while at other places no film was formed. As well, the dose time seems to have an influence on the layer growth. While four cycles at 46 min per cycle resulted in mainly island growth (see arrow Fig. 5), 25 cycles at 6 min per cycle resulted in mainly film growth (see arrow in Fig. 6). This may be due to the preferential chemisorption or decomposition of the precursor at newly nucleated Lu sites: in a long pulse, decomposition carried on with precursor being continually supplied, where with short pulses, once the oxide formed, decomposition of the precursor was less likely.

2. $Lu(TMHD)_3$ and NH_3

For the application of Lu-support particles in a radionuclide generator, an insoluble lutetium-containing layer is needed. LuN is reported to be insoluble in water.[22] Using NH_3 as a coreactant, it is possible to deposit such a coating.[9] Therefore, coating experiments using $Lu(TMHD)_3$ and NH_3 were conducted. The Lu coating results are given in Fig. 7. The Lu deposition is comparable to the coating results using ozone as a coreactant, and again, there was a large spread in the amount of lutetium that is deposited, which is again due to the varying fluidization conditions.
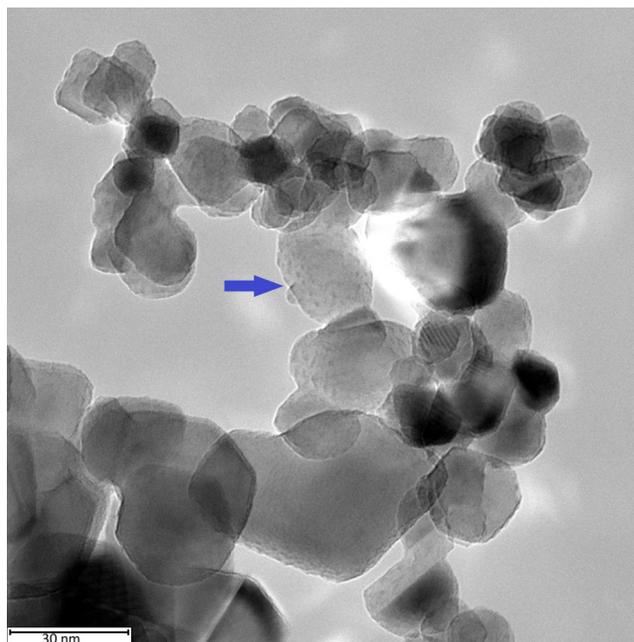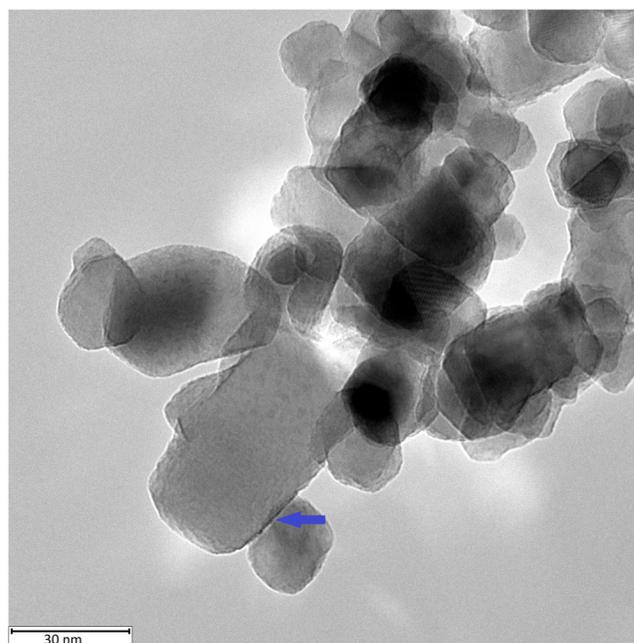
FIG. 6. TEM images of coated particles. 6 min dose time of $Lu(TMHD)_3$ per cycle and 25 cycles, loading 14 wt. % Lu. The arrow indicates the deposited film.
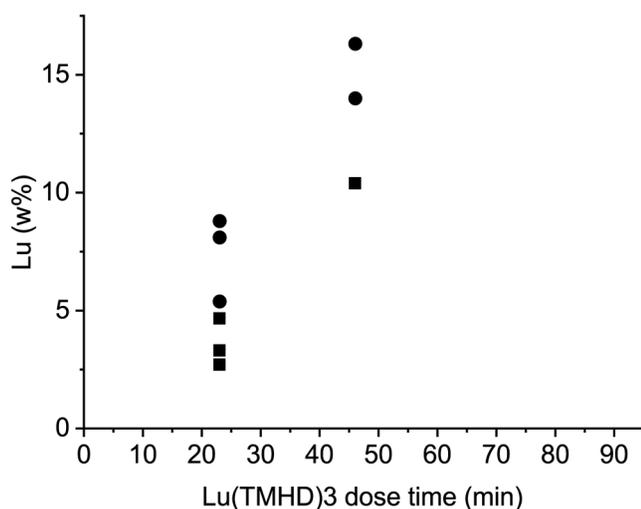
FIG. 7. Lu loading [Lu (wt. %)] as a function of precursor dosing time using Lu $(TMHD)_3$ and NH_3. The circles represent an NH_3 pulse of 10 min while the squares represent an NH_3 pulse of 1 min. Precursor temperature was 210 °C, deposition temperature was 230 °C, and four cycles were applied. The Lu loading was determined by INAA. Because of the widespread results, it was chosen to report the individual experiments rather than the average.

FIG. 8. Lu deposition [Lu (wt. %)] as a function of the precursor dosing time for $Lu(HMDS)_3$ as precursor and ozone coreactant. Precursor temperature was kept at 130 °C while the reactor temperature was at 200 °C. Four cycles were applied. Lu deposition was determined by INAA. Because of the widespread results, it was chosen to report the individual experiments rather than the average.

In order to determine the deposition of N on the particles, XPS measurements were performed on the coated particles. Unfortunately, no N was detected on the particles. First, it was assumed that the amount of N on the particles was too small to be detected, indicating that the amount of NH_3 supplied to the reaction chamber was too low. However, a tenfold increase in the NH_3 pulse still resulted in no N present on the coated particles. This could indicate that the concentration of NH_3 in the coreactant feed is too low (i.e., a conservative concentration was chosen for safety reasons) or that undesired reactions are taking place (i.e., decomposition of NH_3). Guarino et al.[30] reported that TiO_2 is used to reduce NH_3 concentrations in gas flows. This could mean that NH_3 is decomposed at the substrates surface instead of oxidizing the precursor molecules. Future research in our group will be aimed at investigating whether further increasing the NH_3 concentration does clearly lead to LuN deposition.

3. Lu(HMDS)$_3$ and O$_3$

The second precursor that showed potential in the TGA characterization was $Lu(HMDS)_3$. The advantage of using $Lu(HMDS)_3$ over $Lu(TMHD)_3$ is that the coating process can be undertaken at a lower bubbler temperature (130 °C instead of 210 °C). However, $Lu(HMDS)_3$ is more sensitive to oxygen and moisture. Based on the calculated vapor pressure of $Lu(HMDS)_3$ (P_{vap} = 130 Pa; for calculation, see Sec. S1 in the supplementary material)[31] and the same assumptions made for the coating as with $Lu(THMD)_3$, the dosing times for a full monolayer are a 10 min pulse of $Lu(HMDS)_3$ and a 0.81 min pulse of O_3 separated by 10 min purge pulses. These dosing times were taken as the base case. Again, experiments with

other pulse times were conducted to prove self-limiting behavior. The Lu deposition was determined via neutron activation analysis (INAA). For these measurements, the measurement uncertainty was 2% to 7%.

Figure 8 shows that the Lu deposition using $Lu(HMDS)_3$ is much lower compared to $Lu(TMHD)_3$. The most likely explanation for these results is that the precursor decomposed during operation. This possibility was supported by visual inspection of the bubbler showing that the $Lu(HMDS)_3$ precursor had changed color from white to a pale yellow. In addition, the experiment conducted with a freshly filled bubbler showed the higher Lu deposition compared to experiments conducted thereafter.

In previous research by Scarel et al.[12] using $Lu(HMDS)_3$ as a precursor, growth rates up to 0.5 nm/cycle were obtained. The growth rate of our experiments was at least three orders of magnitude lower. It must be noted that Scarel's experiments were conducted on wafers while our experiments were performed on particles. The order of magnitude change in the surface area can have an influence on the deposition rate.

Furthermore, as the TGA already indicated, $Lu(HMDS)_3$ decomposes when in contact with air and moisture as well as when heated up to elevated temperatures. Even though the bubbler was operated at relatively low temperature, prolonged exposure to elevated temperature led to decomposition of the precursor. All in all, $Lu(HMDS)_3$ seems less attractive to be used as an ALD precursor than $Lu(THMD)_3$.

IV. CONCLUSIONS

We have shown that atomic layer deposition of lutetium is possible at atmospheric pressure using a fluidized bed reactor.

The amount of lutetium strongly depends on the precursor chosen. Even though TGA measurements indicated two potential precursors [Lu(HMDS)$_3$ and Lu(TMHD)$_3$], only the latter gave a significant amount of lutetium deposition. Furthermore, proper fluidization of the bed has a strong influence on the amount of Lu deposited on the particles. Also, reproducibility of the system is low. Future research will aim at increased and more constant deposition of Lutetium on particles for use in a radionuclide generator.

AUTHORS' CONTRIBUTIONS

J.L.T.M.M., J.E.B.M.F., and M.B.E.G. investigated this study; B.E.T. performed elemental analysis; original draft was written by J.L.T.M.M.; review and editing of the manuscript done by S.T.B., A.G.D., and J.R.v.O.; and S.T.B., H.T.W., J.R.v.O., and A.G.D supervised this study.

ACKNOWLEDGMENTS

REFERENCES

[1]P. Darmawan, M. Y. Chan, T. Zhang, Y. Setiawan, H. L. Seng, T. K. Chan, T. Osipowicz, and P. S. Lee, Appl. Phys. Lett. **93**, 062901 (2008).

[2]P. Darmawan, P. S. Lee, Y. Setiawan, J. Ma, and T. Osipowicz, Appl. Phys. Lett. **91**, 092903 (2007).

[3]D. Wu, C. Li, Q. Kong, Z. Shi, D. Zhang, L. Wang, L. Han, X. Zhang, and Q. Lin, J. Rare Earths **36**, 819 (2018).

[4]M. R. A. Pillai, S. Chakraborty, T. Das, M. Venkatesh, and N. Ramamoorthy, Appl. Radiat. Isot. **59**, 109 (2003).

[5]D. J. De Vries and H. T. Wolterbeek, Tijdschr. Nucl. Geneesk **34**, 899 (2012).

[6]World Nuclear Association, see: http://www.world-nuclear.org/info/non-power-nuclear-applications/radioisotopes/radioisotopes-in-medicine/. Accessed 24 February 2015.

[7]R. Bhardwaj, A. van der Meer, S. K. Das, M. de Bruin, J. Gascon, H. T. Wolterbeek, A. G. Denkova, and P. Serra-Crespo, Sci. Rep. **7**, 44242 (2017).

[8]European Medicine Agency, "Lutathera, INN-lutetium(177Lu)oxodetreotide—Annex I," EMA/524726/2017, EPAR (2018).

[9]V. Miikkulainen, M. Leskelä, M. Ritala, and R. L. Puurunen, Appl. Phys. Rev. **113**, 021301 (2013).

[10]G. Scarel et al., Appl. Phys. Lett. **85**, 630 (2004).

[11]H. L. Lu, G. Scarel, L. Lamagna, M. Fanciulli, S.-J. Ding, and D. W. Zhang, Appl. Phys. Lett. **93**, 152906 (2008).

[12]G. Scarel et al., J. Electrochem. Soc. **153**, F271 (2006).

[13]M. Roeckerath, T. Heeg, J. M. J. Lopes, J. Schubert, S. Mantl, A. Besmehn, P. Myllymäki, and L. Niinistö, Thin Solid Films **517**, 201 (2008).

[14]D. Kunii and O. Levenspiel, Fluidization Engineering (Elsevier, Stoneham, 2013).

[15]A. W. Weimer, in Carbide, Nitride and Boride Materials Synthesis and Processing, edited by A. W. Weimer (Springer Netherlands, Dordrecht, 1997), pp. 169–180.

[16]D. C. Bradley, J. S. Ghotra, and F. A. Hart, J. Chem. Soc. Dalton Trans. **10**, 1021 (1973).

[17]D. Valdesueiro, G. Meesters, M. Kreutzer, and J. R. van Ommen, Materials **8**, 1249 (2015).

[18]Evonik Industries, "Basic characteristics of AEROSIL fumed silica," https://corporate.evonik.com.

[19]Cas Solutions, see: www.scifinder.cas.org. Accessed 15 March 2016.

[20]D. M. Price, Thermochim. Acta **367–368**, 253 (2000).

[21]S. Barry, paper presented at the ALD 2016, Dublin, Ireland, 2016 (unpublished).

[22]CRC Handbook of Chemistry and Physics, 88th ed., edited by J. R. Rumble (CRC Press, Ohio, 2000).

[23]J. S. Tauster, S. C. Fung, and R. L. Garten, J. Am. Chem. Soc. **100**, 170 (1978).

[24]S. W. Park, J. Woo Kim, H. Jong Choi, and J. Hyung Shim, J. Vac. Sci. Technol. A **32**, 01A115 (2014).

[25]J. Päiväsaari, M. Putkonen, and L. Niinistö, Thin Solid Films **472**, 275 (2005).

[26]T. Boekhoudt, "Technische Universiteit Delft," Master thesis (Technische Universiteit Delft, 2016).

[27]R. L. Puurunen, Chem. Vapor Depos. **9**, 249 (2003).

[28]R. L. Puurunen, J. Appl. Phys. **97**, 121301 (2005).

[29]R. L. Puurunen and W. Vandervorst, J. Appl. Phys. **96**, 7686 (2004).

[30]M. Guarino, A. Costa, and M. Porro, Bioresour. Technol. **99**, 2650 (2008).

[31]See supplementary material at https://doi.org/10.1116/1.5134446 for additional calculations and results.